

Analytical drain current model for amorphous IGZO thin-film transistors in above-threshold regime*

He Hongyu(何红宇)^{1,2,†} and Zheng Xueren(郑学仁)²

¹Faculty of Physics and Optoelectronic Engineering, Guangdong University of Technology, Guangzhou 510006, China

²School of Electronic and Information Engineering, South China University of Technology, Guangzhou 510640, China

Abstract: An analytical drain current model is presented for amorphous In–Ga–Zn–oxide thin-film transistors in the above-threshold regime, assuming an exponential trap states density within the bandgap. Using a charge sheet approximation, the trapped and free charge expressions are calculated, then the surface potential based drain current expression is developed. Moreover, threshold voltage based drain current expressions are presented using the Taylor expansion to the surface potential based drain current expression. The calculated results of the surface potential based and threshold voltage based drain current expressions are compared with experimental data and good agreements are achieved.

Key words: amorphous In–Ga–Zn–oxide (a-IGZO); thin-film transistors (TFTs); surface potential; threshold voltage; trap states

DOI: 10.1088/1674-4926/32/7/074004

PACC: 7340N

EEACC: 2560B

1. Introduction

Amorphous In–Ga–Zn–oxide (a-IGZO) thin-film transistors (TFTs) have been actively researched due to their higher effective mobility than amorphous silicon TFTs and better uniformity than polycrystalline silicon TFTs^[1–3]. An analytical drain current model is important to the applications of a-IGZO TFTs, such as active-matrix liquid-crystal display and peripheral integrated circuit design.

The electrical characteristics of a-IGZO TFTs were mainly dependent on the trap states density within the bandgap. Recently, several techniques to extract the trap states density have been reported^[4,5], and the exponential tail trap state density has been generally accepted. Even though several models have been presented by numerical calculation^[6–10], they were not time efficient and not suitable to circuit simulation. Those available analytical threshold voltage based drain current expressions of a-IGZO TFTs were given by applying the approximate expressions of amorphous silicon TFTs to a-IGZO TFT directly^[11,12]. A surface potential based drain current model for a-IGZO TFTs was not available.

In this paper, a surface potential based drain current expression is developed in the above-threshold regime, assuming an exponential tail trap states density. Charge sheet approximation is applied to derive the surface potential based drain current expression. The surface potential is calculated analytically by the Lambert W equation. In addition, the threshold voltage based drain current expressions are derived using the Taylor expansion. Finally, the calculated results are compared with the experimental data.

2. Surface potential based drain current expression

N-type a-IGZO TFTs with undoped channels are assumed in this paper. In the above-threshold regime, the tail trap states density determines the drain current characteristics of a-IGZO TFTs. The tail trap states density is given by^[4,5]

$$g_{TA}(E) = g_{AD} \exp[(E - E_i)/E_1], \quad (1)$$

where E_i is the intrinsic Fermi level, g_{AD} is the trap states density at E_i , and E_1 is the inverse slope of the trap states density with logarithm scale.

The 1-D Poisson's equation is given by

$$\partial^2\psi/\partial x^2 = (q/\varepsilon_{IGZO})(n + N_{TA}^-), \quad (2)$$

where q is the electron charge, ε_{IGZO} is the dielectric constant of a-IGZO thin films, $n = n_X \exp[(\psi - V_{ch})/\phi_t]$ is the free charge density with $n_X = n_i \exp[(E_{F0} - E_i)/kT]$, $N_{TA}^- = N_{XA} \exp[(\psi - V_{ch})/\phi_1]$ is the trapped charge density with $N_{XA} = g_{AD} \frac{\pi\phi_t}{\sin(\pi\phi_t/\phi_1)} \exp[(E_{F0} - E_i)/E_1]$, n_i is the intrinsic electron density, E_{F0} is the Fermi level in the neutral a-IGZO thin films, which is near the midgap for amorphous TFTs^[13], $\phi_t = kT/q$, $\phi_1 = E_1/q$, k is Boltzmann's constant, T is the temperature, V_{ch} is the quasi-Fermi level, and ψ is the electrical potential vertical to the channels.

From the relationship $2(\partial\psi/\partial x)(\partial^2\psi/\partial x^2) = \partial(\partial\psi/\partial x)^2/\partial x$, one obtains the electric field as

$$F(\psi, V_{ch}) = \partial\psi/\partial x = \left[2 \int_0^\psi (\partial^2\psi/\partial x^2) d\psi \right]^{1/2}. \quad (3)$$

* Project supported by the Cadence Design System, Inc.

† Corresponding author. Email: hehongyu1999@yahoo.com.cn

Received 20 January 2011, revised manuscript received 4 March 2011

Substituting Eq. (2) to Eq. (3), and applying the approximations $\exp(\psi/\phi_t) \gg 1$ and $\exp(\psi/\phi_1) \gg 1$, one obtains

$$F(\psi, V_{ch}) = \sqrt{\frac{2qn_i}{\epsilon_{IGZO}}} \left(\frac{n_X}{n_i} \phi_t \exp \frac{\psi - V_{ch}}{\phi_t} + \frac{N_{XA}}{n_i} \phi_1 \exp \frac{\psi - V_{ch}}{\phi_1} \right)^{1/2}. \quad (4)$$

Applying Gauss's law at the oxide/semiconductor interface, one obtains

$$C_{ox}(V_{GS} - V_{FB} - \psi_s) = \epsilon_{IGZO} F(\psi_s, V_{ch}), \quad (5)$$

where $C_{ox} = \epsilon_{ox}/t_{ox}$, ϵ_{ox} is the gate oxide dielectric constant, t_{ox} is the thickness of gate oxide, V_{FB} is the flat band voltage, and ψ_s is the surface potential.

Substituting Eq. (4) to Eq. (5), one obtains a surface potential equation, as follows,

$$V_{GS} - V_{FB} - \psi_s = \gamma \left(\frac{n_X}{n_i} \phi_t \exp \frac{\psi_s - V_{ch}}{\phi_t} + \frac{N_{XA}}{n_i} \phi_1 \exp \frac{\psi_s - V_{ch}}{\phi_1} \right)^{1/2}, \quad (6)$$

where $\gamma = \sqrt{2q\epsilon_{IGZO}n_i}/C_{ox}$.

From the Pao-Sah model, the trapped charge is given by^[14]

$$Q_t = -q \int_0^{\psi_s} [N_{TA}^-/F(\psi, V_{ch})] d\psi. \quad (7)$$

One should note that the free charge density is much lower than the trapped one in amorphous TFTs^[13]. Ignoring the first term on the right side of Eq. (4), and substituting Eq. (4) to Eq. (7), the trapped charge is approximated as

$$Q_t = -C_{ox}\gamma \left(\frac{N_{XA}}{n_i} \phi_1 \exp \frac{\psi_s - V_{ch}}{\phi_1} \right)^{1/2}, \quad (8)$$

and the free charge is approximated as

$$Q_f = -C_{ox}(V_{GS} - V_{FB} - \psi_s) - Q_t. \quad (9)$$

Using the Taylor expansion to Eq. (6), one obtains

$$V_{GS} - V_{FB} - \psi_s = \gamma \left(\frac{N_{XA}}{n_i} \phi_1 \exp \frac{\psi_s - V_{ch}}{\phi_1} \right)^{1/2} \times \left(\frac{\frac{n_X}{n_i} \phi_t \exp \frac{\psi_s - V_{ch}}{\phi_t}}{\frac{N_{XA}}{n_i} \phi_1 \exp \frac{\psi_s - V_{ch}}{\phi_1}} + 1 \right). \quad (10)$$

Substituting Eqs. (8) and (10) to Eq. (9), one obtains

$$Q_f = -\frac{C_{ox}\gamma n_X \phi_t}{2\sqrt{n_i N_{XA} \phi_1}} \exp \left[\frac{2\phi_1 - \phi_t}{2\phi_1 \phi_t} (\psi_s - V_{ch}) \right]. \quad (11)$$

Since the free charge density is much lower than the trapped one, one can ignore the first term at the right side of Eq. (6) for surface potential calculation, approximately. This approximation is reasonable shown in the textbook, similar to

the surface potential calculation steps for doped c-Si MOSFETs in the subthreshold regime^[14]. One has

$$V_{GS} - V_{FB} - \psi_s = \gamma \left(\frac{N_{XA}}{n_i} \phi_1 \exp \frac{\psi_s - V_{ch}}{\phi_1} \right)^{1/2}. \quad (12)$$

Substituting Eq. (12) to Eq. (11), V_{ch} is eliminated, and one obtains

$$Q_f = -\gamma C_{ox} \xi (V_{GS} - V_{FB} - \psi_s)^{2\phi_1/\phi_t - 1}, \quad (13)$$

where $\xi = \frac{n_X \phi_t \gamma}{2n_i} (\gamma^2 N_{XA} \phi_1 / n_i)^{-\frac{\phi_1}{\phi_t}}$.

The drain current expression in the above-threshold regime is given by^[14]

$$I_{DS} = -\mu_b (W/L) \int_{\psi_{s0}}^{\psi_{sL}} Q_f d\psi_s, \quad (14)$$

where μ_b is the electron-band mobility, W and L are the channel width and length of a-IGZO TFTs, and ψ_{s0} and ψ_{sL} are the surface potential at the source and drain end, respectively. The surface potentials can be calculated analytically from Eq. (12) using the Lambert W function^[15].

Substituting Eq. (13) to Eq. (14), the drain current expression is obtained as

$$I_{DS} = \mu_b (W/L) \gamma C_{ox} \xi \frac{\phi_t}{2\phi_1} \left[(V_{GS} - V_{FB} - \psi_{s0})^{2\phi_1/\phi_t} - (V_{GS} - V_{FB} - \psi_{sL})^{2\phi_1/\phi_t} \right]. \quad (15)$$

3. Threshold voltage based drain current expressions

Noting Eqs. (12) and (15), the threshold voltage is defined as $V_{TH} \approx V_{FB} + \psi_{sTH0}$ when $\psi_{s0TH} = \gamma \left(\frac{N_{XA}}{n_i} \phi_1 \exp \frac{\psi_{s0TH}}{\phi_1} \right)^{1/2}$. In the above threshold regime, $\psi_{s0} \approx \psi_{s0TH}$, $\psi_{sL} \approx \psi_{s0TH} + V_{DS}$, Equation (15) is approximated as

$$I_{DS} = \mu_b \frac{W}{L} \gamma C_{ox} \xi \frac{\phi_t}{2\phi_1} \left[(V_{GS} - V_{TH})^{2\phi_1/\phi_t} - (V_{GS} - V_{TH} - V_{DS})^{2\phi_1/\phi_t} \right]. \quad (16)$$

One should note that, in Ref. [11], the drain current expression is the same as Eq. (16), and Equation (16) is not explicit to effective mobility. Taylor expansion for V_{DS} at $V_{DS} = 0$ is applied to the second term at the right side of Eq. (16), and one obtains

$$(V_{GS} - V_{TH} - V_{DS})^{2\phi_1/\phi_t} = (V_{GS} - V_{TH})^{2\phi_1/\phi_t} - \frac{2\phi_1}{\phi_t} (V_{GS} - V_{TH})^{2\phi_1/\phi_t - 1} V_{DS} + \frac{1}{2} \frac{2\phi_1}{\phi_t} \left(\frac{2\phi_1}{\phi_t} - 1 \right) (V_{GS} - V_{TH})^{2\phi_1/\phi_t - 2} V_{DS}^2. \quad (17)$$

Substituting Eq. (17) to Eq. (16), the drain current expression in the linear regime is developed as

$$I_{DS} = \mu_{AA} C_{ox} \frac{W}{L} (V_{GS} - V_{TH})^{\alpha - 1} \times \left[(V_{GS} - V_{TH}) V_{DS} - \frac{1}{2} \beta V_{DS}^2 \right], \quad (18)$$

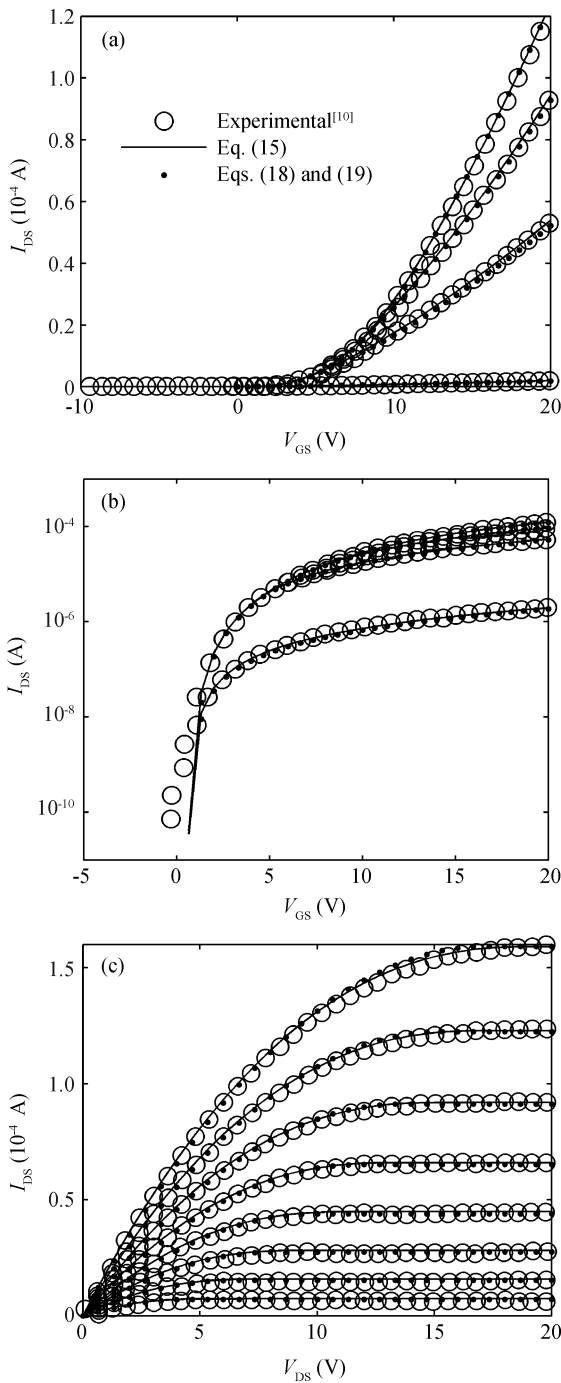


Fig. 1. Comparison of transfer characteristics with (a) linear scale and (b) logarithm scale at different drain voltages, 0.1, 3.1, 6.1, 9.1 V, and (c) output characteristics at different gate voltages, 6, 8, 10, 12, 14, 16, 18, 20 V, between calculated results and experimental data^[10].

where $\mu_{AA} \approx \mu_b \gamma \xi$, $\alpha \approx \frac{2\phi_1}{\phi_t} - 1$, $\beta \approx \alpha$, and the effective mobility $\mu_{eff} = \mu_{AA} (V_{GS} - V_{TH})^{\alpha-1}$. One should note that in Ref. [12], $\beta \approx 0$ is assumed, and it is the approximate formula of Eq. (18).

Using $V_{DSSAT} = (V_{GS} - V_{TH}) / \beta$ to Eq. (18), the drain current expression in the saturation regime is developed as

$$I_{DS} = \frac{1}{2\beta} \mu_{AA} C_{ox} \frac{W}{L} (V_{GS} - V_{TH})^{\alpha+1}. \quad (19)$$

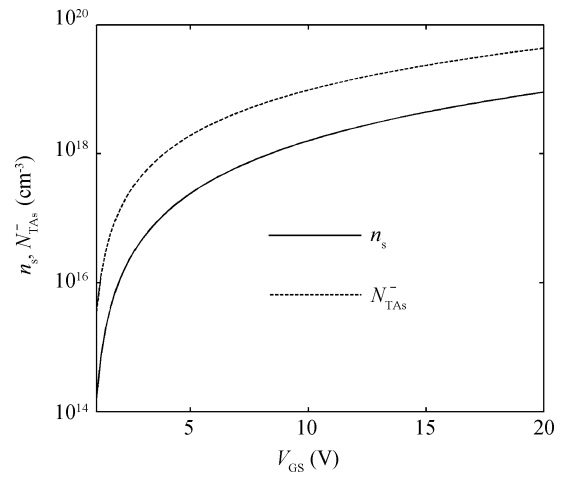


Fig. 2. Calculated free and trapped charge densities at the channel surface of the source end.

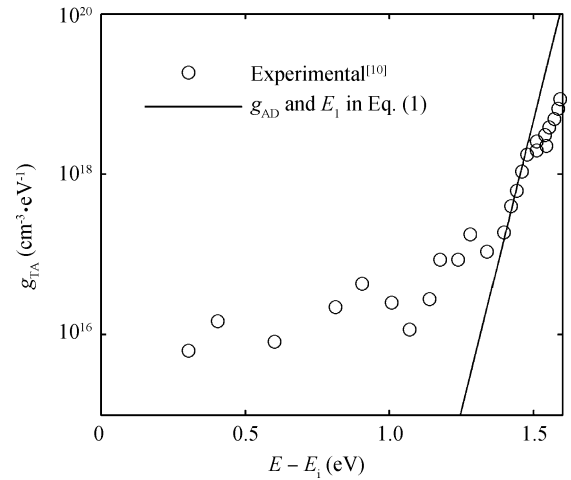


Fig. 3. Comparison of trap states density between parameters in this paper and experimental data.

4. Results and discussions

The experimental data for verification come from Ref. [10]. On a thermally grown SiO₂/Si substrate, the sputtered deposition at RT and the patterning of the Mo gate were followed by the plasma-enhanced chemical vapor deposition (PECVD) of the gate dielectric (SiO₂) at 300 °C. An a-IGZO active layer (In : Ga : Zn = 2 : 2 : 1 at %) was then sputtered by the radio frequency magnetron sputtering at RT in a mixed atmosphere of Ar/O₂^[10].

As shown in Fig. 1, the calculated results from this model are compared with the experimental data^[10], and the parameters for calculation to Eq. (15) are listed as $W = 50 \mu\text{m}$, $L = 30 \mu\text{m}$, $\epsilon_{IGZO} = 11.5 \epsilon_0$ ^[8,16], $\epsilon_{ox} = 3.9 \epsilon_0$, $t_{ox} = 100 \text{ nm}$, $\mu_b = 200 \text{ cm}^2/(\text{V}\cdot\text{s})$, $E_g = 3.2 \text{ eV}$, $E_{F0} = E_i = 0 \text{ eV}$, $N_C = 5 \times 10^{18} \text{ cm}^{-3}$ ^[9], $T = 300 \text{ K}$, $V_{FB} = -0.5 \text{ V}$, $g_{AD} = 930 \text{ m}^{-3}\cdot\text{eV}^{-1}$ and $E_1 = 0.03 \text{ eV}$. The extracted parameters for calculation to Eqs. (18) and (19) are listed as $V_{TH} = 0.9 \text{ V}$, $\alpha = 1.37$, $\beta = 1.11$, $\mu_{AA} = 5.65 \text{ cm}^2/(\text{V}^\alpha\cdot\text{s})$.

From the caption of Eq. (2), $n_s = n_X \exp(\psi_s/\phi_t)$ and $N_{TA_s}^- = N_{XA} \exp(\psi_s/\phi_1)$ are the free and trapped charge den-

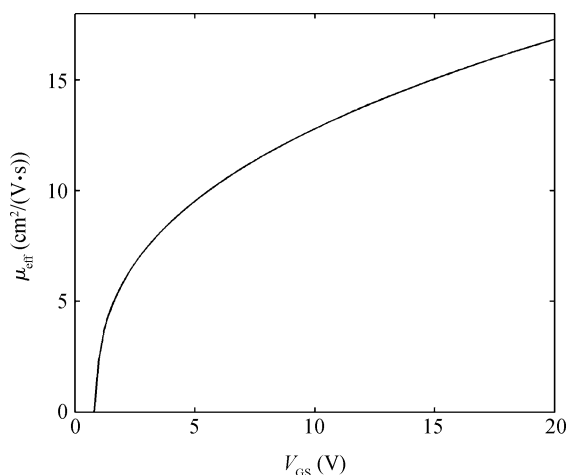


Fig. 4. Calculated effective mobility of a-IGZO TFTs.

sities at the channel surface of source end, respectively. As shown in Fig. 2, the previous assumption, that the free charge density is much lower than the trapped one in amorphous TFTs, is reasonable. In addition, the tail trap states density for calculation in this paper is compared with the experimental data shown in Fig. 3. Moreover, the calculated effective mobility is shown in Fig. 4, and the value of effective mobility is reasonable for a-IGZO TFTs^[8].

However, as shown in Fig. 1(b), this work cannot fit the experimental data of subthreshold current because the deep trap state density is not taken into account. In addition, the deep trap states were seriously affected by the interface trap states^[17]. Even with this limitation, good agreements were obtained in the above-threshold regime shown in Fig. 1.

5. Conclusion

Surface potential based and threshold voltage based drain current expressions have been presented for a-IGZO TFTs in the above-threshold regime, assuming an exponential tail trap states density within the bandgap. The drain current expressions are analytical and suitable for circuit simulation.

References

- [1] Kamiya T, Nomura K, Hosono H. Present status of amorphous In–Ga–Zn–O thin-film transistors. *Sci Technol Adv Mater*, 2010, 11(4): 044305
- [2] He H, Zheng X. Analytical model of undoped polycrystalline silicon thin-film transistors consistent with Pao–Sah model. *IEEE Trans Electron Devices*, 2011, to be published
- [3] Deng W, Zheng X. Modeling of self-heating effects in polycrystalline silicon thin film transistors. *Journal of Semiconductors*, 2009, 30(7): 074002
- [4] Park J H, Jeon K, Lee S, et al. Extraction of density of states in amorphous GaInZnO thin-film transistors by combining an optical charge pumping and capacitance–voltage characteristics. *IEEE Electron Device Lett*, 2008, 29(12): 1292
- [5] Lee S, Park S, Kim S, et al. Extraction of subgap density of states in amorphous GaInZnO thin-film transistors by using multifrequency capacitance–voltage characteristics. *IEEE Electron Device Lett*, 2010, 31(3): 231
- [6] Hsieh H H, Kamiya T, Nomura K, et al. Modeling of amorphous InGaZnO₄ thin film transistors and their subgap density of states. *Appl Phys Lett*, 2008, 92(13): 133503
- [7] Jeon K, Kim C, Song I, et al. Modeling of amorphous InGaZnO thin-film transistors based on the density of states extracted from the optical response of capacitance–voltage characteristics. *Appl Phys Lett*, 2008, 93(18): 182102
- [8] Park J H, Lee S, Jeon K, et al. Density of states-based DC I – V model of amorphous gallium–indium–zinc–oxide thin-film transistors. *IEEE Electron Device Lett*, 2009, 30(10): 1069
- [9] Fung T C, Chuang C S, Chen C, et al. Two-dimensional numerical simulation of radio frequency sputter amorphous In–Ga–Zn–O thin-film transistors. *J Appl Phys*, 2009, 106(8): 084511
- [10] Jeon Y W, Kim S, Lee S, et al. Subgap density-of-states-based amorphous oxide thin film transistor simulator (DeAOTS). *IEEE Trans Electron Devices*, 2010, 57(11): 2988
- [11] Shin J H, Hwang C S, Cheong W S, et al. Analytical modeling of IGZO thin-film transistors based on the exponential distribution of deep and tail states. *Journal of the Korean Physical Society*, 2009, 54(1): 527
- [12] Fung T C, Abe K, Kumomi H, et al. Electrical instability of RF sputter amorphous In–Ga–Zn–O thin-film transistors. *Journal of Display Technology*, 2009, 5(12): 452
- [13] Shur M, Hack M. Physics of amorphous silicon based alloy field-effect transistors. *J Appl Phys*, 1984, 55(10): 3831
- [14] Arora N D. MOSFET models for VLSI circuit simulation. New York: Springer-Verlag, 1993
- [15] Corless R M, Gonnet G H, Hare D E G, et al. On Lambert’s W function. *Adv Comput Math*, 1996, 5(1): 329
- [16] Lee S, Park J H, Jeon K, et al. Modeling and characterization of metal–semiconductor–metal-based source–drain contacts in amorphous InGaZnO thin film transistors. *Appl Phys Lett*, 2010, 96(11): 113506
- [17] Erslev P T, Sundholm E S, Presley R E, et al. Mapping out the distribution of electronic states in the mobility gap of amorphous zinc tin oxide. *Appl Phys Lett*, 2009, 95(19): 192115